4-Dimensional Electrical Resistivity Tomography for continuous, near-real time monitoring of a landslide affecting transport infrastructure in British Columbia, Canada

Jessica Holmes[1,2*], Jonathan Chambers[2], Philip Meldrum[2], Paul Wilkinson[2], James Boyd[2,3], Paul Williamson[2], David Huntley[4], Kelvin Sattler[5], David Elwood[5], Vinayagamoothy Sivakumar[1], Helen Reeves[2], Shane Donohue[6]

[1]Queen's University Belfast, Belfast, United Kingdom

[2]British Geological Survey, Nottingham, United Kingdom

[3]Lancaster University, Lancaster, United Kingdom

[4]Geological Survey of Canada, Vancouver, British Columbia, Canada

[5]University of Saskatchewan, Saskatoon, Saskatchewan, Canada

[6]University College Dublin, Dublin, Ireland

[*]Corresponding author email: jeho@bgs.ac.uk

Acknowledgments

Data Availability Statement

Abstract

The Ripley Landslide is a small (0.04 km^2), slow-moving landslide in the Thompson River Valley, British Columbia, that is threatening the serviceability of two national railway lines. Slope failures in this area are having negative impacts on railway infrastructure, terrestrial and aquatic ecosystems, public safety, communities, local heritage, and the economy. This is driving the need for monitoring at the site, and in recent years there has been a shift from traditional geotechnical surveys and visual inspections for monitoring infrastructure assets toward less invasive, lower cost, and less time-intensive methods, including geophysics. We describe the application of a novel electrical resistivity tomography (ERT) system for monitoring the landslide. The system provides near-real time geoelectrical imaging, with results delivered remotely via a modem, avoiding the need for costly repeat field visits, and enabling near-real time interpretation of the 4D ERT data. Here, we present the results of the ERT monitoring alongside field sensor-derived relationships between suction, resistivity, moisture content, and continuous monitoring single-frequency GNSS stations. 4-D ERT data allows us to monitor spatial and temporal changes in resistivity, and by extension, in moisture content and soil suction. The models reveal complex hydrogeological pathways, as well as considerable seasonal variation in the response of the subsurface to changing weather conditions, which cannot be predicted through interrogation of weather and sensor data alone, providing new insight into the subsurface processes active at the site of the Ripley Landslide.

Key words

Electrical resistivity tomography, hydrogeophysics, landslide

Introduction

Landslides on the transport network represent a major social, economic, and environmental challenge, and long-term monitoring of unstable slopes that affect transport infrastructure is desirable to support the management and maintenance decisions required to maintain the serviceability of the transport network. This is particularly important in light of environmental change (IPCC, 2014), which is likely to affect precipitation patterns around the globe and may have a destabilising effect on slopes in close proximity to transport networks. As the demand placed on the global transport network increases with growing global population, at the same time as the challenge of environmental change emerges, there is a clear need to monitor slopes and to mitigate against failure.

Traditional monitoring techniques used on the transport network include visual inspection and geotechnical surveys. Visual inspection is commonly used to assess the condition of slopes, whereby surface expressions of failure are observed (such as tension cracks) (Power et al., 2016; Smethurst et al., 2017). However, slope surfaces are often obscured by vegetation, and visual inspections provide limited insight into subsurface processes, which are vital to understanding the mechanisms for slope failure. Furthermore, these surface expressions of failure often occur too late for mitigation measures to be implemented. Intrusive geotechnical sampling provides information about the subsurface and allows material behaviour to be characterised (Fell et al., 2000). However, they are costly and invasive, as they typically involve boreholes, trenches, and penetration tests, and only provide information about discrete points within the region of interest. Hence, in geologically

3

heterogeneous areas, geotechnical surveys provide little insight into the complex behaviours, hydrogeological pathways, and movement characteristics of the slopes. Recently, there has been a shift toward using geophysical methods for monitoring unstable slopes (Whiteley et al., 2019) and slopes that affect transport infrastructure specifically (Chambers et al., 2014; Gunn et al., 2015; Chambers et al., 2016; Bergamo et al., 2016a and b).

Electrical resistivity provides information on lithology, with mineralogy and porosity (and by extension, density) influencing resistivity. Resistivity is also sensitive to moisture content (Waxman and Smits, 1968), changing resistivity of the pore fluid (Archie, 1942), and temperature (Hayley et al., 2007), and changes can be monitored over time. Geoelectrical monitoring is particularly useful in its application to managing slopes that affect transport infrastructure, owing to the relationships between resistivity, moisture content, and suction (Merritt et al., 2016). Given that moisture content and suction are important factors governing slope stability due to their controls on effective stress and shear strength (Lu et al., 2010), geoelectrical monitoring can provide insight into the complex hydrogeological pathways active in unstable slopes, and where movement data is also available, moisture and suction thresholds for movement can be developed (Uhlemann et al., 2017).

Study area – The Ripley Landslide, British Columbia, Canada

Since the late 19th Century, landslides along a 10 km stretch of Thompson River valley (Figure 1) – a vital railway transportation corridor in British Columbia, Canada – have caused damage to infrastructure, and threatened public safety, potable water supplies, and salmon runs. Efforts to understand and characterise landslide mechanisms and behaviour in the area

4

have been focussed on the Ripley Landslide since 2013 (Bobrowsky et al., 2014; Huntley et al., 2014; Macciotta et al., 2014; Huntley et al., 2017; Huntley et al., 2019).

The Ripley Landslide is a small, slow-moving (3-55 mm/year (Bunce and Chadwick, 2012)), translational landslide. Slope failure at this site is unlikely to be catastrophic, but movement is sufficient to cause settlement of the railway tracks at the toe of the slide, such that tracks need to be lifted and additional ballast added beneath them, to allow for the continued safe passage of freight and passenger trains (Huntley et al., 2017). Therefore, there is a demand for slope monitoring at the site of the Ripley landslide, with a long-term aim of developing moisture thresholds for the prediction of slope movement.

An extensive programme of geophysical monitoring, which commenced in 2013, has provided critical information on the subsurface geology and hydraulic pathways, vital to understanding the processes contributing to slope instability. Both terrestrial and waterborne geophysical surveys were carried out, including: Electrical Resistivity Tomography (ERT), Ground Penetrating Radar (GPR), Fixed Frequency Electromagnetic Induction (FEM), Seismic Refraction, Multichannel Analysis of Surface Waves (MASW), and Acoustic Bathymetry (Huntley et al., 2017; Huntley et al., 2019). This data is complemented by displacement monitoring data (InSAR, Global Positioning System (GPS), Fibre Optic monitoring) (Bunce and Chadwick, 2012; Bobrowsky et al., 2014; Huntley et al., 2014; Macciotta et al., 2014).

A reconnaissance ERT survey was carried out in November 2013, which consisted of three lines running E-W, 50 m apart, and two lines running NE-SW, 10 m apart. An IRIS Instruments Syscal R1 Plus was used with a Wenner array of 48 electrodes, and a 5 m electrode spacing (Huntley et al., 2017). This survey covered the full extent of the Ripley

Landslide, and provided initial insight into the geological setting of the landslide, and formed the context for this research.

This paper describes the use of a novel ERT monitoring system PRIME – Proactive Infrastructure Monitoring and Evaluation (Huntley et al., 2019) – for developing greater insights into the hydrogeological pathways of the slope, building upon the information garnered from previous geophysical surveys. Here, we present 4-D ERT models developed from two years of monitoring at the Ripley Landslide (from November 2017 to November 2019). This monitoring data is presented in the context of the wider geological setting of the landslide, as revealed through the development of a 3-D ground model, and shows the complex pathways for active groundwater flow in the landslide, affecting slope stability. New insights into the hydrogeological regime of the Ripley landslide are made possible through the long-term monitoring of the slope, advancing the understanding of the factors controlling slope stability in this important transportation corridor.

Methodology

3-D Ground model development

Landslide processes can be extremely complex, particularly in highly heterogeneous earthwork slopes, and in order to best comprehend these processes, an understanding of the subsurface geology of the active slopes is required (Merritt et al., 2014). 3-D ground models can provide this by combining a range of site data, including aerial photographs, borehole logs, geological surveys, and more recently, geophysical and laboratory data (Fookes, 1997; Tye et al., 2011; Merritt et al., 2014; Thornton et al., 2018). Individually, each of these data inputs provides only a snapshot of the site. For example, LiDAR and aerial photographs only give surface topography information, and boreholes provide discrete point information about

the subsurface, and whilst ERT data can provide broad spatial and volumetric information, this is only in areas that have been directly surveyed, which is not often the whole of a site owing to cost restraints. However, when each of these data inputs are combined together, a more holistic picture of a field site can be developed, allowing for a greater understanding of how the geology of the site influences the processes affecting the slope stability (Fookes, 1997; Griffiths et al., 2012).

Here, an integrated approach was taken to developing a 3-D ground model of the Ripley Landslide: the model was developed using GOCAD software designed to digitize borehole logs and geological cross-sections in the context of baseline images such as georeferenced Digital Elevation Models (DEMs) and aerial photographs (Mallet, 1992). Inputs into the ground model presented here include a DEM of the site, extending beyond the area of the active landslide, borehole information, ERT data from previous surveys and from ongoing monitoring, and previous interpretations of the geology of the area based on geophysical surveys (Huntley et al., 2017). The DEM of the site provides detailed insight into the surface geomorphology of the landslide. Stratigraphic boundaries were identified by combining borehole data with geophysical data. This allowed for improved interpretation of the PRIME data, and provided insight into the subsurface structure of the landslide.

ERT data from the PRIME system installed on the Ripley landslide, and from ERT surveys carried out on the site in November 2013 were both used to improve the interpretation of the geology. As shown in Figure 2, the reconnaissance ERT surveys span a larger area than those of the PRIME system, which sets the PRIME data in the context of the wider landslide area. The 2013 ERT survey data were reprocessed using the same workflow as the PRIME data to ensure the resulting models were consistent with the PRIME models. Lithological boundaries were interpreted from the geophysical boundaries present in the resulting ERT models, and

7

were corroborated by previous geological interpretations of the Thompson River Valley (e.g. Eshraghian et al., 2007; Huntley and Bobrowsky, 2014).

Time-lapse ERT monitoring

In November 2017, a PRIME system was installed at the site of the Ripley Landslide. The installation consists of sensor arrays connected to the PRIME system, which takes electrical resistivity measurements at set time intervals (twice per day in this case), and sends the data to a remote server via an internet connection, allowing the site to be monitored continually through time (Gunn et al., 2015) to develop a 4-D ERT dataset. The PRIME system consists of two sensor arrays; one 91 m long with 45 evenly-spaced, buried rod electrodes, oriented NE-SW across the slope, and crossing the head scarp at the southern end; and one 54 m long with 27 evenly-spaced, buried rod electrodes, oriented SE-NW downslope, and spanning the eastern extent of the head scarp. Contact resistances of the electrodes were low in summer, with minimum, maximum, average, and standard deviation (in brackets) values of 290 Ω, 1750 Ω, and 820 Ω, (290 Ω) respectively. Winter contact resistances were higher owing to localised freezing at the surface of the slope, with minimum, maximum, average, and standard deviation of 1300 Ω, 14000 Ω, and 6000 Ω (2400 Ω) respectively. The workflow of the PRIME system is presented in Figure 3.

The need for repeat field visits is reduced by the continual and automated data collection, offering a major advantage of such systems over traditional ERT surveys. It also results in a far greater temporal resolution than manual repeat ERT surveys can provide; measurements are currently taken every 12 hours at the Ripley site. This allows for a more detailed interrogation of the response of the subsurface to short-timescale changes in external forcing factors, including temperature, precipitation, and river level, all of which are important controls on the stability of the Ripley Landslide (Eshraghian et al., 2007; Hendry et al., 2015;

8

Journault et al., 2018). The 4-D ERT images provide information about the seasonal changes in subsurface hydrology, which will be vital in furthering the understanding of slope behaviour, failure characteristics, and subsurface hydrology of the Ripley landslide, and other landslides in the Thompson River valley that also threaten the integrity of vital railway infrastructure.

4-D ERT inversion

Initially, the raw data measured by the PRIME system was filtered to ensure that the data used would produce an accurate model of the subsurface. This involved removing data points with high contact resistances (>10 kΩ). Measurements with negative transfer resistance were also removed from the dataset. Forward and reciprocal measurements were taken, which allow reciprocal errors to be calculated. This is important as poorly estimated measurement errors can lead to over- or under-fitting of the data to a model during geophysical inversion (Tso et al., 2017), and the use of error models based on reciprocity helps to assess the measurement errors more accurately. Measurements with large reciprocal errors (>5%) were filtered out of the dataset, and the forward and reciprocal values for each measurement were averaged and used to produce error models for each data set in the time-lapse inversion (Lesparre et al., 2017).

On average, up to May 2019, 7.47% of the data had reciprocal errors greater than 5%, and was filtered out of the data set prior to inversion. Post-May 2019, this increased to an average of 44%. The reason for this increase in reciprocal error is currently unknown; there have been no obvious changes in contact resistances on site, or in the magnitude of the current supplied, nor is the error concentrated around any particular electrodes. This may be indicative of a system issue, and investigations are ongoing. However, the remaining data still seem to be sufficient to produce reasonable models.

The data were inverted using an iteratively reweighted Gauss–Newton least-squares method (Res3DInvX64 from Geotomo Software) (Loke, 2017) with an L1 norm on the data misfit, an L1 spatial smoothness constraint and an L2 temporal smoothness constraint. This optimization method reduces the difference between measured and calculated resistivity values by adjusting the resistivity of the model blocks (Loke et al., 2003). This difference is given by the RMS error (root-mean-squared error), and the model iteration selected as the best model is generally the model in which the RMS error undergoes very little change (2-5%) from one model iteration to the next.

Weekly data between December 2017 and December 2019 were combined into a single time-lapse data set and inverted simultaneously using an L2 temporal smoothness constraint to ensure the resistivity changed in a smooth manner with time (Kim et al., 2009; Loke et al., 2014). The data for each of the two lines were inverted separately, in 3-D. A 3-D inversion was used for three reasons: i) It allows for offline variations in topography, which is not flat; ii) The lines are not straight; iii) The inversion is able to better capture online and offline 3-D effects where they are present. The resulting 3-D models were then clipped so that only the regions directly below the lines were displayed.

Temperature correction is necessarily part of the inversion workflow here because seasonal variations in temperature can result in changes to the subsurface resistivity that are in the same order as the changes induced by moisture content variations (Uhlemann et al., 2017). Indeed, where temperature exceeds 0°C, resistivity decreases linearly by approximately 2% per °C increase in temperature (Hayley et al., 2007). As such, each resistivity image presented here has been corrected for the influence of temperature, in order to avoid misinterpretation of the data. This was done by fitting a simple temperature model, as a function of time and depth (Chambers et al., 2014), to data from temperature sensors in the

air and at five different depths in the slide mass. It was assumed that this model was valid at all positions in the monitoring area and that the coupling coefficient was -2% per °C throughout the subsurface.

Field-sensor measurements

Point sensors are located across the slope, close to the PRIME system (Figure 2); two boreholes instrumented with TEROS 21 soil suction sensors were installed in November 2017 at the head scarp of the landslide, covering a range of depths from 0 to 2 m below the surface. These allow field-based relationships between suction and resistivity (from the PRIME data) to be established. Soil suction (negative pore water pressure) increases the shear strength of the soil and contributes to overall slope stability (Fredlund et al., 1978), so near-surface changes in suction in response to changes in weather conditions are an important consideration for slope stability assessment. There is a close relationship between suction and moisture content in terms of the soil water characteristic curve (SWCC) (Fredlund and Xing, 1994), with soil suction increasing non-linearly with decreasing moisture content, and displaying hysteresis through wetting and drying cycles. There is also a relationship between resistivity and moisture content, as resistivity also increases with decreasing moisture content (e.g., Uhlemann et al., 2017). As such, it is possible to derive relationships between resistivity and suction measured independently in the field (Crawford and Bryson, 2017). However, it should be noted that when derived from field measurements, these are indirect relationships, owing to the differences in the volume of the subsurface that is measured in each case (Piegari and Di Maio, 2013).

Here, the soil suction measured by the TEROS 21 soil suction sensors in the field was related to the resistivity in the same location by isolating cells in the PRIME resistivity models. Firstly, a mask was applied to the model data that isolated the cells in the immediate vicinity

of the soil suction sensor, and then the average resistivity of these cells was calculated for each time step in the model. This allows for the development of a field-based relationship between resistivity and soil suction, which will enable the validation of laboratory-based petrophysical relationships in future work.

Surface change detection measurements

In 2016, an experimental Global Navigation Satellite System (GNSS) was installed at the Ripley Landslide to provide better spatial and temporal coverage of surface displacement. Twelve Geocubes - small, rugged, single-frequency, high-resolution (millimetric) GNSS receivers with directional antennas - relayed geospatial data to a Geocoordinator hosting a proprietary operating system developed and serviced by Ophelia Sensors in France. A fixed Geocube was installed on stable bedrock confining the landslide in the northeast; the remaining eleven were positioned across the slide body to capture spatial variation in displacement (Figure 4). A 3G network modem and an omnidirectional antenna connected the Geocoordinator to the internet, allowing 24-hour offsite access to Geocube data.

Results and discussion

3-D Ground model

A 3-D ground model for the Ripley Landslide is presented in Figure 4. This sets the PRIME arrays in the context of the wider field site, and reveals the geological setting of the landslide and surrounding areas, allowing slope failure behaviour to be better characterised and understood. This is important not only for the Ripley Landslide, which itself threatens the integrity and serviceability of two national railway lines, but also for the management of

other landslides along the Thompson River Valley, many of which are much larger than the Ripley slide.

The volume of the landslide monitored by the PRIME system, and therefore of greatest interest to this research, is dominated by three main lithological units: fine-grained glacial deposits (Unit 3 and Unit 4), and coarse-grained post-glacial sediments (Unit 8). This information will guide future laboratory work, which will focus on characterising and developing petrophysical relationships for these units. It is also useful in the context of understanding the landslide mechanics, which are intrinsically linked to the slope material characteristics. The slip surface of the landslide is likely to be restricted to the unsaturated zone (above the water table) in the region of the slope monitored by the PRIME system, resulting in negative pore water pressures (suction), which is important for the behaviour of slope material and in assessing slope stability.

Unit 3 is a glaciolacustrine clay composed of finely laminated clay-silt couplets (varves) (Clague and Evans, 2003). There is considerable variation in the material properties within this unit, as shown in Table 1. The unit is characterised by fine grain sizes (predominantly silts and clays). Unit 3 is the lithological unit in which the shear surface of the Ripley Landslide lies.

Unit 4 is interpreted as lodgement till deposited during the Late Wisconsinan Fraser Glaciation (Clague and Evans, 2003; Eshraghian et al., 2007; Huntley and Bobrowsky, 2014). This material is a silt-rich diamicton, as evidenced by the results of particle size analysis of the material (Table 1).

Unit 8 is interpreted as post-glacial material and is characterised by coarse colluvial sediments (Table 1), deposited by the Thompson River (Clague and Evans, 2003; Eshraghian et al., 2007).

In addition to the subsurface structures revealed by the 3-D ground model, surface features are also observed. The topographic information allowed for identification of key geomorphological structures, including the location of the head scarp and side scarps of the landslide, tension cracks traversing the surface of the slide, and gullies upslope of the landslide.

Time-lapse ERT

The baseline image of the landslide from December 2017 (Figure 5) shows the resistivity profile of the site, and the dominant lithological units (coarse alluvial Unit 8 sediments overlying high-plasticity glaciolacustrine Unit 3 sediments and Frasier glaciation Unit 4 diamicton) and key features of the landslide are demarcated. An inferred shear surface is presented, although it should be noted that the ERT has been unable to resolve the exact location of the shear surface of the landslide as there is no geophysical contrast either side of the shear surface, given that it occurs within a single lithological unit. Time lapse images are shown in Figure 6, with a monthly snapshot of the changes in resistivity (%) from the December 2017 baseline. The chosen constraints used in the data inversion were found to produce convincing results in the top few metres of the model, although where the model resolution is low (e.g. at depth) it is possible that the L2 temporal constraint could be causing the changes to overshoot, producing possibly spurious changes in resistivity at depth.

The changes in resistivity due to moisture content changes and due to freezing and melting of pore water across the slope vary both in time and space, highlighting the utility of long-term monitoring of landslides. The spatial heterogeneity in moisture content changes and the distribution of hydrogeological pathways revealed by the 4-D ERT models are particularly interesting, as these subsurface patterns of moisture movement cannot be captured using monitoring techniques traditionally used by asset owners to monitor slopes that affect transport infrastructure.

Seasonal changes in the moisture and frozen or liquid state distribution of the slope are evident: In the winter months, the slope is dryer, although some areas that show an increase in resistivity are more likely associated with localised freezing than with drying. During the spring, at the onset of the snow melt season, there is a large decrease in resistivity, particularly at the surface of the slope and along key hydrogeological pathways, associated with an increase in moisture content.

Of particular note is the evolution of a wetting front along the head scarp of the landslide during the snow melt season, highlighted in Figure 6. This is associated with a decrease in resistivity, following a period of increased resistivity linked to localised freezing at the surface of the slope. To demonstrate this hydrogeological regime, the average resistivity of the active layer of the slope was calculated for each time step in the PRIME monitoring, as shown in Figure 7. Resistivity increases throughout the winter months, as the slope dries and freezes periodically. A decrease in resistivity occurs in the spring, corresponding to the start of the snowmelt season. Ground thawing also releases frozen pore water. This is in contrast to the hydrogeological regime of the slope that would be predicted based on rainfall data alone, as the wetting of the slope occurs during periods of negative effective rainfall (net rainfall when accounting for evapotranspiration (Blaney and Criddle, 1962)).

15

In addition to responding to changes in moisture content, there is also a strong resistivity response to changes in air temperature. Following the onset of freezing (sub 0°C) air temperature, with a phase lag of approximately 2 weeks, there is a sharp drop in resistivity, followed by a sharp rise (Figure 7). A similar response is recorded by Krautblatter et al. (2010) and by Wu et al. (2017); resistivity drops as temperatures fall below 0°C during a supercooling phase, followed by nucleation of ice and a self-induced increase in soil temperature due to latent heat emission, which causes spontaneous freezing associated with a sharp rise in resistivity.

As such, in areas where temperature plays an important role in determining the hydrogeological response of the subsurface to changing weather conditions, geoelectrical monitoring can provide insights inaccessible through interrogation of rainfall data alone.

Field-based petrophysical relationships

The relationship between soil suction and resistivity measured in the field (using the soil suction sensors and long-term monitoring data from the PRIME system installed on site) is shown in Figure 8. The resistivity data presented here are the average resistivity of the cells of the PRIME model proximal to the suction sensors from 0 to 2 m depth, and the suction data are the average readings of the suction sensors for the range of depths, although the results are dominated by the sensor closest to the surface (30 cm depth) as these data have the largest magnitude of suctions. There is a clear relationship between suction and resistivity at the Ripley Landslide; suction increases as resistivity increases. Both parameters show similar seasonal trends and respond cyclically to changing weather conditions (Figure 8a). This is due to the non-linear relationship of suction with moisture content, and the close correlation of moisture content with resistivity. The relationship between suction and resistivity shown in Figure 8b has a Pearson correlation coefficient of 0.64, suggesting a moderate-to-strong

16

correlation. In future work, this relationship will be further developed in the laboratory, using material from key lithological units (Units 3, 4 and 8).

Field-based geospatial relationships

Eight Geocubes installed across Ripley Landslide were recording 3-D displacement from November 2018 to June 2019, while three units were not active due to wildlife damage or low battery charge. Geocubes in proximity to the PRIME array capture movement at varying rates (Figure 9), indicative of displacement of multiple slide blocks along moderately steep-dipping slide planes. The most northerly block monitored moved horizontally NW 5.55 cm, while dropping 1.8 cm in elevation. At the NE end of the PRIME array, the graben block moved NW 4.5 cm with a 1.7 cm drop in elevation. The central block captured by the intersection of NE-SW and SE-NW arrays, moved horizontally NW 5.0 cm, dropping 1.5 cm over the eight-month trial (Figure 9).

Over the summer and autumn, Geocubes record minimal horizontal displacement, and small (<1 cm) uplift and subsidence events in response to antecedent precipitation events and seasonal temperature changes as indicated by PRIME and weather station data (Figure 9). This period of stability is associated with high river levels, which, in combination with the low-permeability of the landslide materials, results in buttressing of the submerged portions of the toe slope while groundwater is at its maximum level in the slide body. High river levels also result in an increase in the mobilized shear strength of the slope, with increasing effective stress along the sliding surface, thereby increasing slope stability (Macciotta et al., 2014; Hendry et al., 2015; Schafer et al., 2015). The greatest displacement rates detected by Geocubes occur during winter and spring when the river levels are low, as this buttressing effect is removed from the toe of the landslide. This also coincides with the timing of the development of the wetting front down the slip face of the landslides (Figure 6), so the

17

increase in displacement is likely due to a combination of debuttressing, along with elevated pore pressures in the slip face as snow melts and saturates the slope.

Conclusions and future work

Detailed information on the subsurface processes at the Ripley landslide has been made available through a new 4-D ERT dataset, advancing the interpretations made based on previous monitoring efforts. The development of a 3-D ground model from geophysical datasets, borehole data, and geological mapping reveals a complex geological setting for the Ripley Landslide, and highlights the need for geophysical investigation in such sites where highly heterogeneous subsurface structures cannot be identified using traditional earthworks monitoring techniques such as visual surveys and discrete-point geotechnical investigations.

4-D geoelectrical monitoring of the Ripley landslide reveals complex hydrogeological pathways, which respond seasonally to changing weather conditions. Single-frequency GNSS sensors capture seasonal changes in the amounts and rates of surface displacement across the PRIME installation related to subsurface hydrogeophysical events. Notably, the response of the subsurface to changing weather conditions is controlled to a greater extent by temperature than by rainfall at the Ripley landslide. While short-term responses to rainfall are observed in the spatial and temporal evolution of the hydrogeological regime at the site, the greatest changes are seen seasonally, with resistivity responding strongly to the influence of snowmelt as a result of fluctuating surface temperatures. This highlights the utility of geoelectrical monitoring for assessing slope stability as it enables a detailed understanding of the soil moisture pathways and spatial heterogeneities that cannot be identified using traditional asset monitoring techniques. A clear relationship between resistivity and soil suction is measured in the field, demonstrating the utility of geoelectrical monitoring for assessing the integrity of

18

unstable slopes, since soil suction (negative pore water pressure) plays a role in determining slope stability.

Future work will focus on the calibration of the timelapse resistivity models with laboratory-derived petrophysical relationships. Laboratory experiments will enable direct relationships between resistivity, moisture content and suction to be established for each of the key geological units present in the monitored area of the slope, which will then be applied to the resistivity models using the 3-D ground model as a basis for the identification of different geological units. These calibrated models will then be coupled with other in situ sensor data and movement data, and used to identify precursors to failure such that the PRIME system can be used actively in slope management on the Ripley Landslide.

Figure Legends

Table 1. Characteristics of the predominant lithological units in the PRIME-monitored section of the Ripley Landslide (units 3, 4 and 8).

		Unit 3	Unit 4	Unit 8
Geology	Lithology	Glaciolacustrine varves	Glacial diamicton (Till)	Colluvial gravels
Atterberg Limits	Liquid Limit, %	59.5±7.6	37.5	36.5
	Plastic Limit, %	24.8±1.8	24.5	26.3
Particle Size Analysis	Gravel, %	0.6±0.6	4.6	16.2
	Sand, %	2.3±1.8	14.7	54.5
	Silt, %	42.0±8.8	44.9	18.4
	Clay, %	55.0±10.2	35.8	10.9

Figure 1. Location of the Thompson River valley, south-central British Columbia. a) Location of the Thompson River valley area of interest (white rectangle). b) Thompson River Valley, showing locations of landslides (red dots), and the Ripley Landslide (red star).
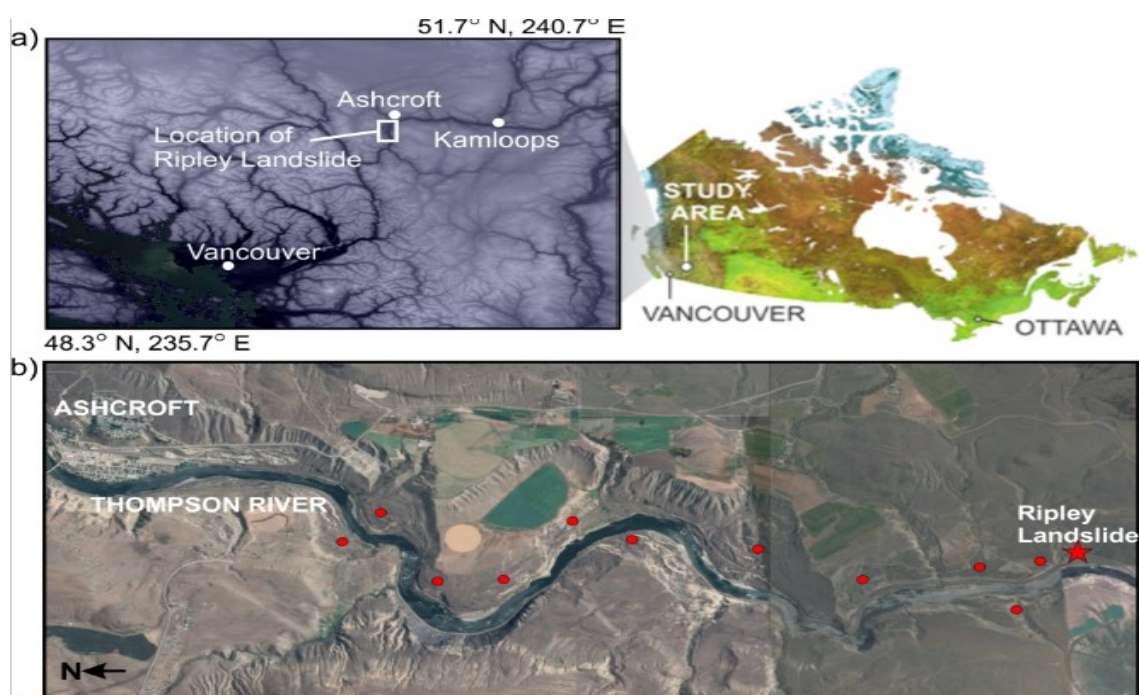
Figure 2 a) Overview of geophysical surveys carried out on the Ripley Landslide, including the previous reconnaissance ERT survey carried out in 2013 (yellow lines), and PRIME infrastructure shown by the red lines. The locations of boreholes, suction meters, and point sensor measurements are also shown. Key features of the landslide are marked in black. b) Weather station installed in 2016, and continuously recording climate variables since then.
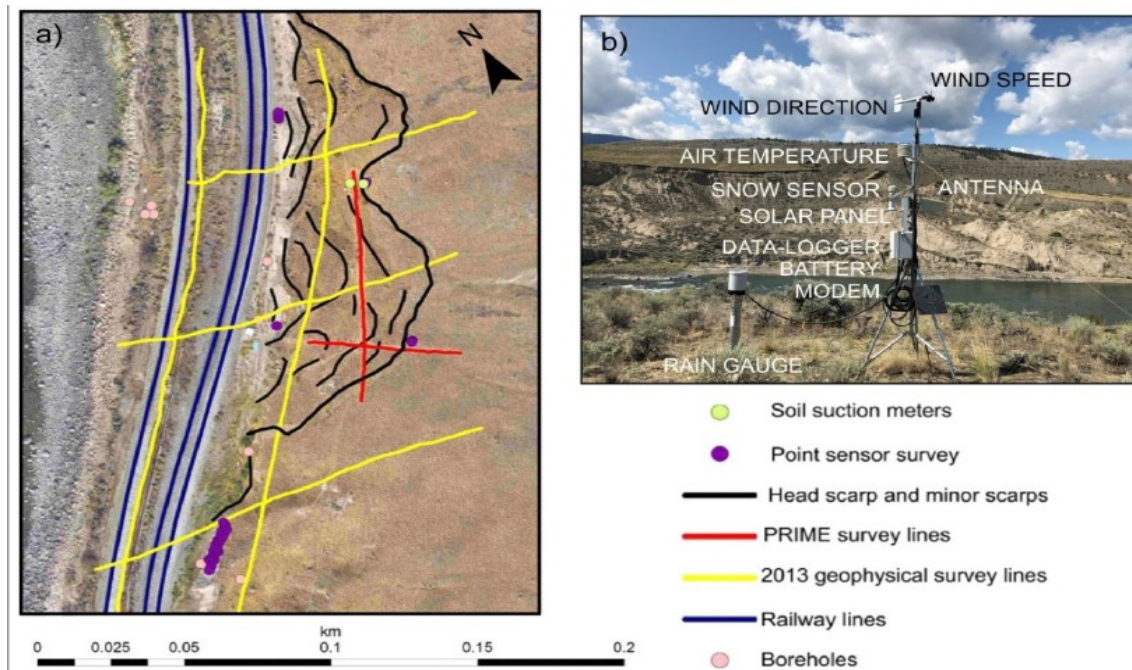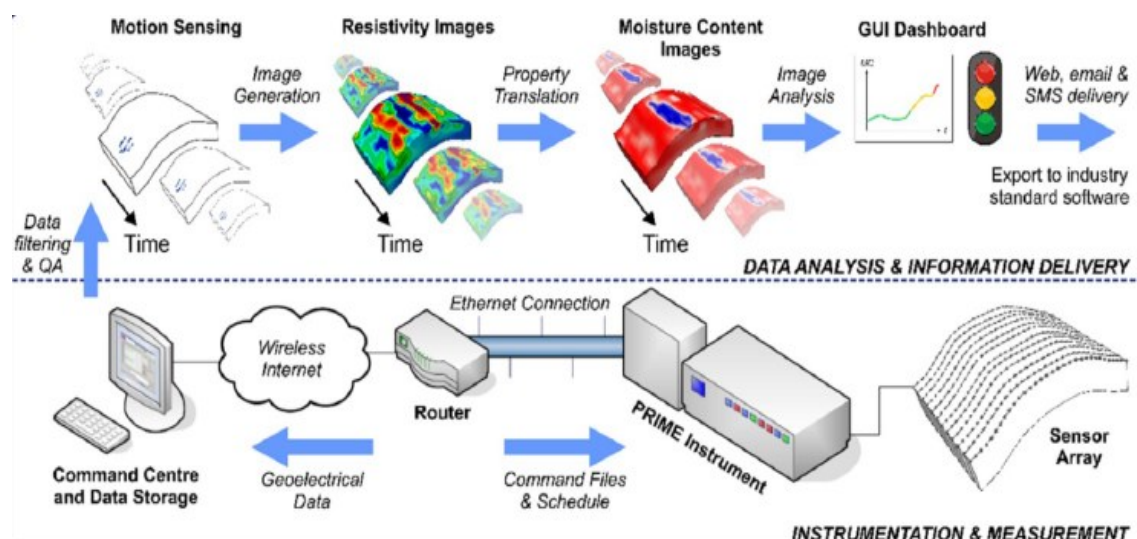

Figure 3. Workflow of the PRIME system.

Figure 4. a) Geomorphology map of the Ripley landslide, including the locations of the landslide head scarp, tension cracks, terrace scarp, and gullies. The locations of boreholes, and the railway lines are also shown. b) shows the terrestrial reconnaissance ERT survey images from 2013 (lines A-E), setting the wider context for the PRIME ERT lines (1 and 2).
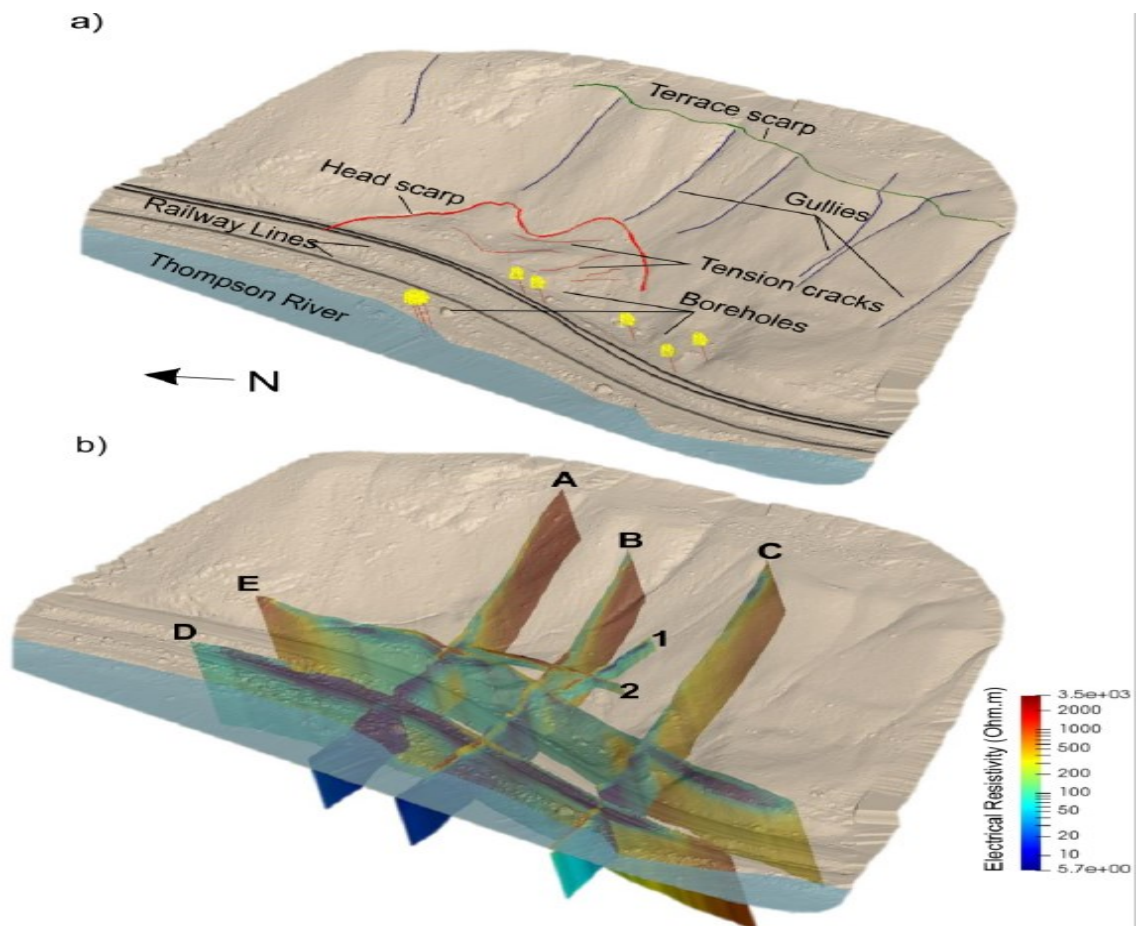
Figure 5. Baseline resistivity model of PRIME monitoring, from 05/12/2017. Different lithological units are demarcated by the black lines, and key features of the landslide are highlighted. The location of the soil suction sensor is also shown. An inferred failure surface is shown by the white dashed line; the spacing of the dashes increases with depth as the location of the failure surface becomes less certain.
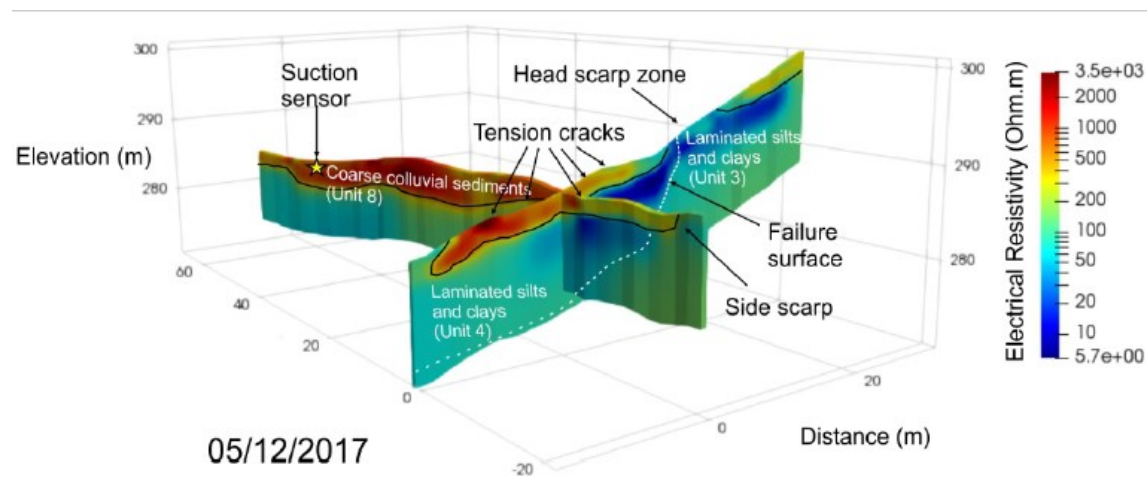

Figure 6. Time series of models produced from the 4-D monitoring of the Ripley Landslide. Change in resistivity (%) is shown relative to the baseline resistivity model from December 2017 (shown in Figure 5).
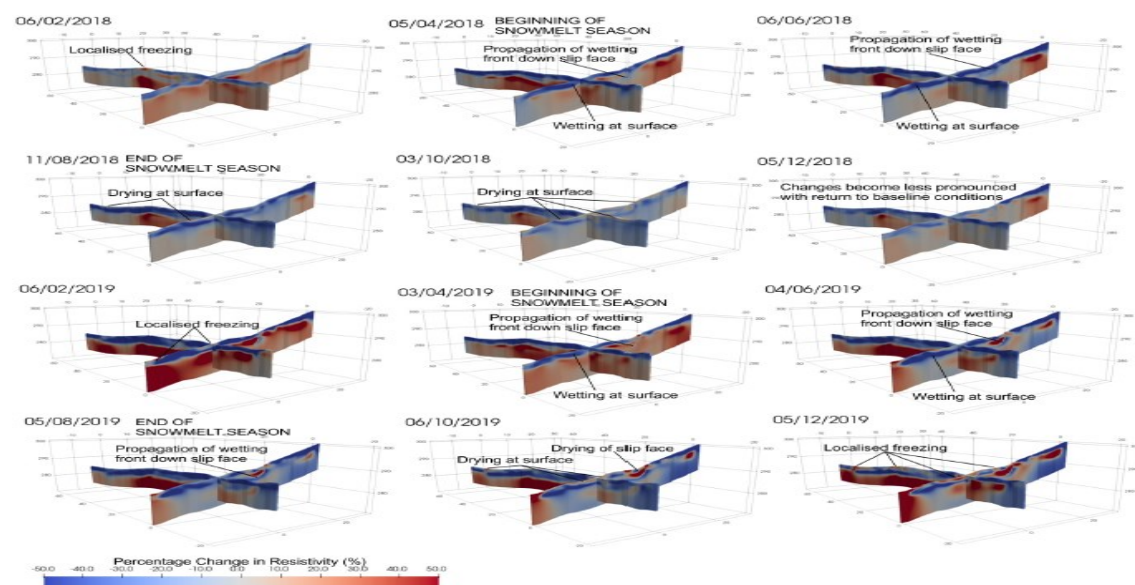
Figure 7. Average resistivity of the hydrologically active surface layer of the Ripley landslide over time, shown alongside weather data over the same period.
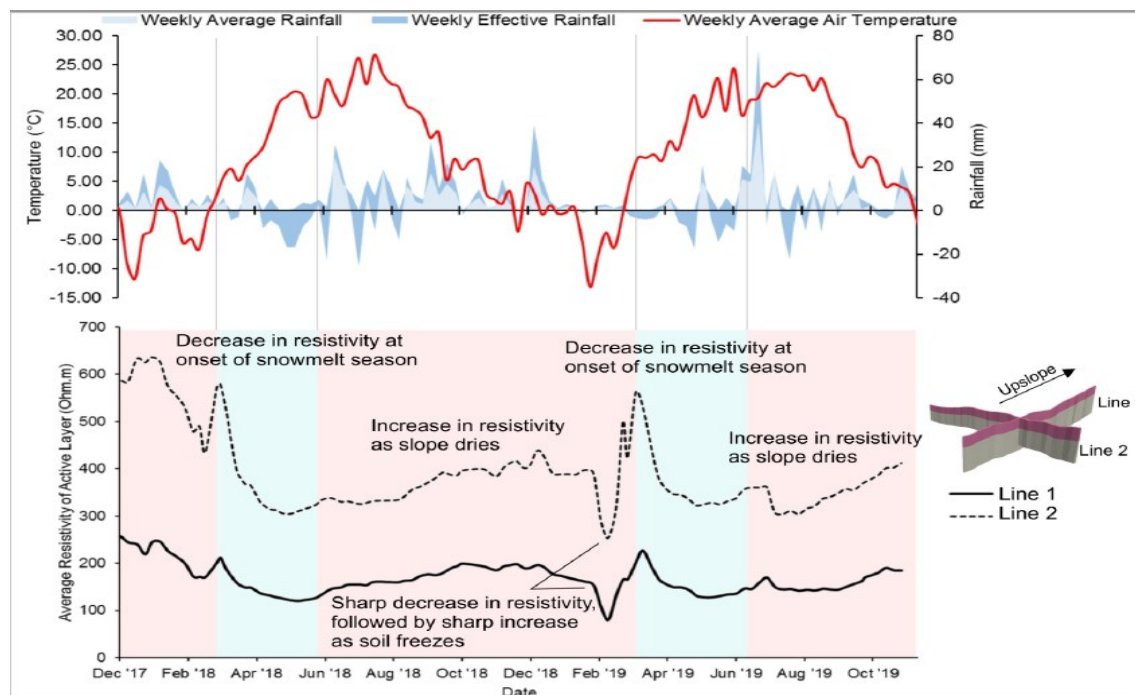

Figure 8. Relationship between resistivity (from PRIME monitoring) and suction (from point sensors installed on the slope) data. a) shows the variation in resistivity (black markers) and suction (white markers) through time, and b) shows the field-based relationship between resistivity and suction.
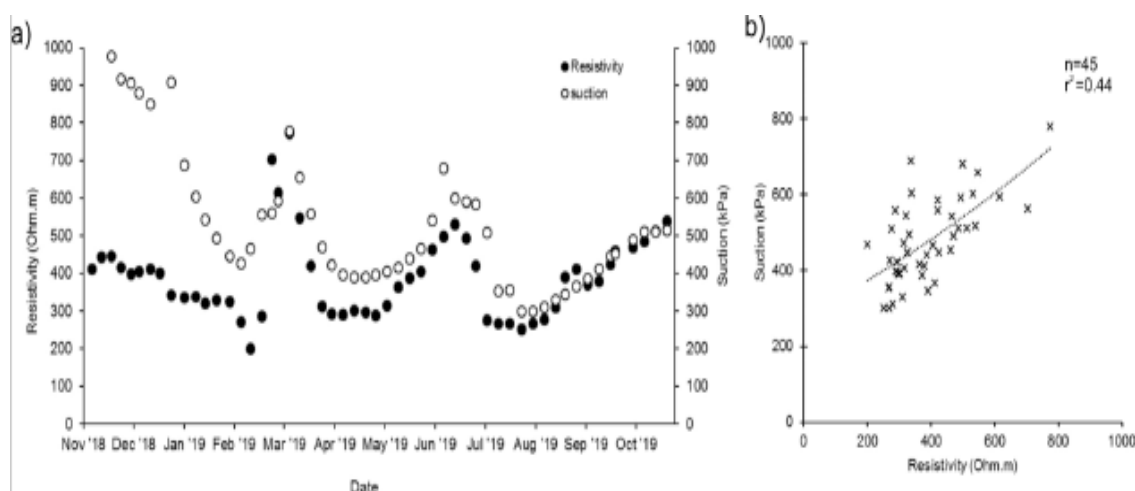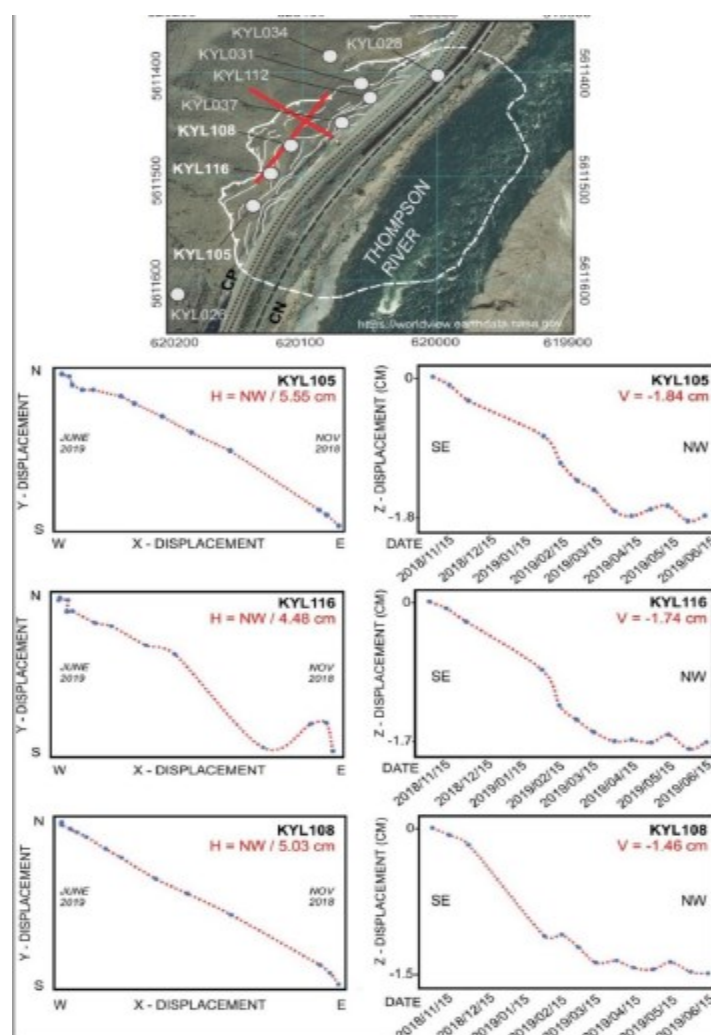
24

Figure 9. Geocube displacement results: X,Y - horizontal displacements trends, and Z - vertical displacements (cm) for November 11, 2018 to June 04, 2019.

References

Archie, G.E. (1942) The electrical resistivity log as an aid in determining some reservoir characteristics. *Transactions of the American Institute of Mining, Metallurgical and petroleum Engineers.* 146, 54- 62.

Bergamo, P., Dashwood, B., Uhlemann, S., Swift, R., Chambers, J. E., Gunn, D. A. & Donohue, S. (2016a). Time-lapse monitoring of climate effects on earthworks using surface waves. Geophysics. 81. EN1-EN15.

Bergamo, P., Dashwood, B., Uhlemann, S., Swift, R., Chambers, J. E., Gunn, D. A.. Donohue, S. (2016b) Time-lapse monitoring of fluid-induced geophysical property variations within an unstable earthwork using P-wave refraction. Geophysics. 81. EN17-EN27.

Blaney, H. F. and Criddle, W. D. (1962) Determining consumptive use and irrigation water requirements. U.S. Department of Agriculture. Agricultural Research Service Technical Bulletin 1275

Bobrowsky, P. T., Sladen, W., Huntley, D., Zhang, Q., Bunce, C., Edwards, T., Hendry, M., Martin, D., Choi, E. (2014) Multi-parameter monitoring of a slow moving landslide: Ripley Slide, British Columbia, Canada. In: Engineering Geology for Society and Territory – Volume 2 Landslide Processes, edited by G. Lollino, D. Giordan, G. Battista Crosta, J. Corominas, R. Azzam, J. Wasowski and N. Sciarra; p. 155-159. IAEG (International Association of Engineering Geology and the Environment) Congress, Turin, Italy 15 – 19 September 2014, Springer Publishing (Contribution #20140007)

Bunce, C. and Chadwick, I. (2012) GPS monitoring of a landslide for railways. In Eberhardt et al. (Editors), Landslides and Engineered Slopes: Protecting Society through Improved Understanding. 1373-1379.

Chambers, J. E., Gunn, D. A., Wilkinson, P. B., Meldrum, P. I., Haslam, E., Holyoake, S., Kirkham, M., Juras, O., Merritt, A., Wragg, J. (2014) 4D electrical resistivity tomography monitoring of soil moisture dynamics in an operational railway embankment. Near Surface Geophysics. 12. 61-72.

Chambers, J. E., Meldrum, P. I., Wilkinson, P. B., Gunn, D., Uhlemann, S., Kuras, O., Swift, R., Inauen, C., Butler, S. (2016) Remote Condition Assessment of Geotechnical Assets Using a New Low-power ERT Monitoring System. Near Surface Geoscience 2016, 22nd European Meeting of Environmental and Engineering Geophysics. Engineering Geology and Geotechnical Investigations V. 4th September.

Clague, J. J. and Evans, S. G. (2003) Geological framework of large historic landslides in Thompson River Valley, British Columbia. Environmental Engineering Geoscience. 9. 201–212.

Crawford, M. & Bryson, L. (2017) Assessment of active landslides using field electrical measurements. Engineering Geology. 233.

Eshraghian, A., Martin, C. D., Cruden, D. M. (2007) Complex Earth Slides in the Thompson River Valley, Ashcroft, British Columbia. The Geological Society of America. 13 (2). 161-181.

Fell, R., Hungr, O., Leroueil, S., Riemer, W. (2000) Keynote Lecture – Geotechnical Engineering Of The Stability Of Natural Slopes, And Cuts And Fills In Soil. International

Society for Rocks and Mechanics. ISRM International Symposium, 19-24 November, Melbourne, Australia.

Fredlund, D, G., Morgenstern, N, R., Widger, R. A. (1978) The shear strength of unsaturated soil. Canadian Geotechnical Journal. 15. 313-321.

Fredlund, D. G. & Xing, A. (1994) Equations for the soil-water characteristic curve. Canadian Geotechnical Journal. 31, 521-532.

Fookes, P. G. (1997) Geology for engineers: the geological model, prediction and performance. Quarterly Journal of Engineering Geology and Hydrogeology. 30. 293-424.

Griffiths, J. S., Stokes, M., Stead, D. & Giles, D. (2012) Landscape evolution and engineering geology: results from IAEG Commission 22. Bulletin of Engineering Geology and the Environment. 71. 605-636.

Gunn, D. A., Chambers, J. E., Uhlemann, S., Wilkinson, P. B., Meldrum, P. I., Dijkstra, T. A., Haslam, E., Kirkham, M., Wragg, J., Holyoake, S., Hughes, P. N., Hen-Jones, R., Glendinning, S. (2015) Moisture monitoring in clay embankments using electrical resistivity tomography. Construction and Building Materials.

Hayley, K., Bentley, L. R., Gharibi, M. & Nightingale, M. (2007) Low temperature dependence of electrical resistivity: Implications for near surface geophysical monitoring. Geophysical Research Letters. 34 (18).

Hendry, M. T., Macciotta, R., Martin, C. D. & Reich, B. (2015). Effect of Thompson River elevation on velocity and instability of Ripley Slide. Canadian Geotechnical Journal, 52, 257-267.

Huntley, D. and Bobrowsky, P. (2014) Surficial geology and monitoring of the Ripley Slide, near Ashcroft, British Columbia, Cananda. Geological Survey of Canada. Open File 7531.

Huntley, D., Bobrowsky, P., Qing, Z., Sladen, W., Bunce, C., Edwards, T., Hendry, M., Martin, D., Choi, E. (2014) Fiber optic strain monitoring and evaluation of a slow-moving landslide near Ashcroft, British Columbia, Canada. In: Landslide Science for a Safer Geoenvironment. Edited by K. Sassa, P. Canuti and Y. Yin. 1. 415-422. Springer Verlag. 3rd World Landslide Forum (ICL-IPL), Beijing, China 2 – 6 June 2014. (Contribution #20150019)

Huntley, D., Bobrowsky, P., Parry, N., Bauman, P., Candy, C., Best, M. (2017) Ripley Landslide: the geophysical properties of a slow-moving landslide near Ashcroft, British Columbia. Geological Survey of Canada. Open File 8062.

Huntley, D., Bobrowsky, P., Hendry, M., Macciotta, R., Elwood, D., Sattler, K., Best, M., Chambers, J., Meldrum, P. (2019) Application of multi-dimensional electrical resistivity tomography datasets to investigate a very slow-moving landslide near Ashcroft, British Columbia, Canada. Landslides, 16 (5). 1033-1042.

IPCC (2014) Climate Change 2014: Synthesis Report. Contribution of Working Groups I, II and III to the Fifth Assessment Report of the Intergovernmental Panel on Climate Change [Core Writing Team, R.K. Pachauri and L.A. Meyer (eds.)]. IPCC, Geneva, Switzerland, 151 pp.

Journault, J., Macciotta, R., Hendry, M., Charbonneau, F., Huntley, D. and Bobrowsky, P. (2018) Measuring displacements of the Thompson River valley landslides, south of Ashcroft, B.C., Canada, using satellite InSAR. Landslides. 15 (4). 621-636.

Kim, J. H., Yi, M. J., Park, S. G., Kim, J. G. (2009) 4-D inversion of DC resistivity monitoring data acquired over a dynamically changing earth model. *Journal of Applied Geophysics*. 68. 522–532.

Krautblatter, M., Verleysdonk, S., Flores-Orozco, A., Kemna, A. (2010) Temperature-calibrated imaging of seasonal changes in permafrost rock walls by quantitative electrical resistivity tomography (Zugspitze, German/Austrian Alps) *Journal of Geophysical Research. Earth Surface.* 115 (F2).

Lesparre, N., Nguyen, F., Kemna, A., Robert, T., Hermans, T., Daoudi, Flores-Orozco, A. (2017) A new approach for time-lapse data weighting in electrical resistivity tomography, Geophysics 82, E325-E333

Loke, M. H., Acworth, I. and Dahlin, T. (2003) A comparison of smooth and blocky inversion methods in 2D electrical imaging surveys. Exploration Geophysics. 34. 182-187.

Loke, M. H., Dahlin, T., Rucker, D. F. (2014) Smoothness-constrained time-lapse inversion of data from 3-D resistivity surveys. *Near Surface Geophysics*. 12. 5-24.

Loke, M. H. (2017) RES3DINVx64 ver. 4.07 with multi-core and 64-bit support for Windows XP/Vista/7/8/10. Rapid 3-D Resistivity & IP inversion using the least-squares method. Geoelectrical Imaging 2-D and 3-D. Geotomo Software.

Lu, N., Godt, J. W., Wu, D. T. (2010) A closed- form equation for effective stress in unsaturated soil. Water Resources Research. 46 (5). W05515.

Macciotta, R., Hendry, M., Martin, D., Elwood, D, Lan, H., Huntley, D., Bobrowsky, P., Sladen, W, Bunce, C., Choi, E, Edwards, T. (2014) Monitoring of the Ripley Slide in the

Thompson River Valley, B.C. Proceedings of Geohazards 6 Symposium, Kingston, Ontario, Canada

Mallet, J., L. (1992) GOCAD: A Computer Aided Design Program for Geological Applications. In: Turner A.K. (eds) Three-Dimensional Modeling with Geoscientific Information Systems. NATO ASI Series (Series C: Mathematical and Physical Sciences), vol 354. Springer, Dordrecht

Merritt, A. J., Chambers, J. E., Murphy, W., Wilkinson, P. B., West, L. J., Gunn, D. A., Meldrum, P. I., Kirkham, M., Dixon, N. (2014) 3D ground model development for an active landslide in Lias mudrocks using geophysical, remote sensing and geotechnical methods. Landslides. 11 (4). 537-550.

Merritt, A. J., Chambers, J. E., Wilkinson, P. B., West, L. J., Murphy, W., Gunn, D., Uhlemann, S. (2016) Measurement and modelling of moisture—electrical resistivity relationship of fine-grained unsaturated soils and electrical anisotropy. Journal of Applied Geophysics. 124. 115-165.

Piegari, E. and Di Maio, R. (2013) Estimating soil suction from electrical resistivity. Natural Hazards Earth System Sciences. 2369–2379.

Power, C., Mian, J., Spink, T., Abbott, S., Edwards, M. (2016) Development of an Evidence-based Geotechnical Asset Management Policy for Network Rail, Great Britain. Procedia Engineering. 143. 726-733.

Schafer, M., Macciotta, R., Hendry, M., Martin, D., Bobrowsky, P., Huntley, D., Bunce, C., Edwards, T. (2015) Instrumenting and Monitoring a Slow Moving Landslide. GeoQuebec. 7p.

Smethurst, J. A., Smith, A., Uhlemann, S., Wooff, C., Chambers, J., Hughes, P., Lenart, S., Saroglou, H., Springman, S. M., Löfroth, Hughes, D. (2017) Current and future role of instrumentation and monitoring in the performance of transport infrastructure slopes. Quarterly Journal of Engineering Geology and Hyrdogeology. 50. 271-286.

Thornton, J. M., Mariethoz, G. & Brunner, P. (2018) A 3D geological model of a structurally complex Alpine region as a basis for interdisciplinary research. Scientific Data. 5. 180238.

Tso, C. H. M., Kuras, O., Wilkinson, P. B., Uhlemann, S., Chambers, J. E., Meldrum, P. I., Graham, J., Sherlock, E.F., Binley, A. (2017) Improved characterisation and modelling of measurement errors in electrical resistivity tomography (ERT) surveys. Journal of Applied Geophysics. 146. 103-119.

Tye, A.M., Kessler, H., Ambrose, K., Williams, J.D.O., Tragheim, D., Scheib, A., Raines, M., Kuras, O. (2011) Using integrated near-surface geophysical surveys to aid mapping and interpretation of geology in an alluvial landscape within a 3D soil-geology framework. Near Surface Geophysics. 9 (1). 15-31.

Uhlemann, S., Chambers, J., Wilkinson, P., Maurer, H., Merritt, A., Meldrum, P., Kuras, O., Gunn, D., Smith, A., Dijkstra, T. (2017) Four-dimensional imaging of moisture dynamics during landslide reactivation. Journal of Geophysical Research: Earth Surface. 122 (1). 398-418.

Waxman, M. H., Smits, L. J. M. (1968) Electrical conductivities in oil- bearing shaly sands. *Society of Petroleum Engineers Journal*. 8, 107- 122.

Whiteley, J., Chambers, J., Uhlemann, S., Wilkinson, P. & Kendall, J. (2019) Geophysical Monitoring of Moisture-Induced Landslides: A Review. Reviews of Geophysics. 57 (1). 106-145.

Wu, Y., Nakagawa, S., Kneafsey, T, J., Dafflon, B., Hubbard, S. (2017) Electrical and seismic response of saline permafrost during freeze – thaw transition. *Journal of Applied Geophysics*. 146. 16-26.